Diffusion Imaging of the Prostate at 3.0 Tesla

Peter Gibbs, PhD, Martin D. Pickles BHS (Hons), and Lindsay W. Turnbull, MD

Objectives: We sought to assess the efficacy of diffusion imaging in the differential diagnosis of prostatic carcinoma using a 3.0 T scanner and parallel imaging technology.

Materials and Methods: Diffusion-weighted images were acquired using a single shot echo-planar imaging sequence with $b = 0$ and 500 seconds/mm^2. Apparent diffusion coefficient (ADC_y) values were calculated in tumor and healthy-appearing peripheral zone for 62 patients. Diffusion tensor images were also acquired in 25 patients and mean diffusivity and fractional anisotropy determined.

Results: Significant differences were noted between prostatic carcinoma ($1.33 \pm 0.32 \times 10^{-3}$ mm^2/s) and peripheral zone ($1.86 \pm 0.47 \times 10^{-3}$ mm^2/s) for ADC_y. Significant differences between the 2 tissue types were also noted for mean diffusivity and fractional anisotropy. Utilizing a cut-off of 1.45×10^{-3} mm^2/s for mean diffusivity, a sensitivity of 84% and a specificity of 80% were obtained.

Conclusions: Diffusion imaging of the prostate was implemented at high magnetic field strength. Reduced ADC and increased fractional anisotropy values were noted in prostatic carcinoma.

Key Words: prostate cancer, diffusion imaging, echo-planar imaging

(*Invest Radiol* 2006;41: 185–188)

Prostate cancer is one of the commonest forms of malignancy in men with an incident rate that has risen dramatically during the last few years. This increase is primarily as a result of the increasing prevalence in the younger-than 65 age group.[1] Management of prostatic carcinoma is guided by digital rectal examination in combination with prostate-specific antigen (PSA) blood testing and histopathologic grade of biopsy specimens. However, the efficacy of PSA blood testing is known to be poor, with high false-positive and false-negative rates.[2]

Magnetic resonance imaging (MRI) of prostate cancer is primarily used to differentiate patients with organ confined disease from patients with locally infiltrative disease extending beyond the prostatic capsule. Despite its excellent soft-tissue contrast, the overlapping characteristics of prostatitis and prostatic carcinoma in the peripheral zone and of benign prostatic hyperplasia (BPH) and prostatic carcinoma in the central gland result in MRI having a reduced histologic specificity. Although high-resolution T2 maps have been shown to be indicative of the citrate concentration in the prostate and thus the presence of prostatic carcinoma,[3] accurate assessment of tumor volume using MRI has proved to be problematic.[4–6]

The use of functional methods, such as dynamic contrast-enhanced (DCE) MRI, diffusion-weighted imaging (DWI), or spectroscopic imaging, has been recommended as potential complements to conventional imaging.[7] DCE-MRI provides potential insight into a tissue's vascularity, reduced apparent diffusion coefficient (ADC) values are indicative of increased cellularity or areas of cell swelling after the loss of energy-dependent sodium pumps, and spectroscopic imaging enables determination of citrate content—the absence of which is believed to represent areas of prostatic carcinoma.

It has been suggested that MRI of the prostate can be used in the monitoring and/or prediction of treatment effects after hormonal therapy and/or radiotherapy.[8] For example, Buckley et al[9] have invested considerable effort in establishing baseline physiology and MR characteristics of the prostate for eventual use as prognostic indicators. DWI also may be a potentially useful tool in treatment assessment as demonstrated in small animal models.[10–12] Using a Dunning rat AT6/22 prostate tumor implanted subcutaneously in nude mice, Dodd and Zhao detected radiotherapy-induced changes in the ADC value of as much as 110%.[10] Plaks et al[12] used a subcutaneous human prostate adenocarcinoma xenograft to observe a biphasic ADC change in response to treatment with photodynamic therapy.

A number of recent articles have demonstrated the feasibility of DWI in the human prostate,[13–17] and some success has been reported in differentiating cancerous and noncancerous areas of peripheral zone tissue using calculated ADC values.[14,16,17] Although these works concentrated on establishing the mean diffusivity, there are some early indications of potential anisotropy within the prostate gland.[13,18] By quantifying the trace elements of the diffusion tensor, Gibbs et al[13] demonstrated increased diffusion in the superior–inferior direction compared with the transaxial plane. A very recent work[19] used diffusion tensor imaging (DTI) of the prostate gland to assess fractional anisotropy in the central gland and peripheral zone for a group of 6 healthy volunteers. However, because these data were obtained at 1.5 T, a clinically unacceptable acquisition time of 15 minutes was necessary to

Received June 23, 2005 and accepted for publication, after revision, October 8, 2005.

From the Centre for MR Investigations, Division of Cancer, Postgraduate Medical School, University of Hull, Hull, United Kingdom.

Supported by Yorkshire Cancer Research.

Reprints: Dr Peter Gibbs, PhD, Centre for MR Investigations, Hull Royal Infirmary, Anlaby Road, Hull HU3 2JZ, United Kingdom. E-mail: p.gibbs@hull.ac.uk.

ISSN: 0020-9996/06/4102-0185

obtain images of sufficient signal-to-noise ratio (SNR). Indeed, this problem can be said to have beset all previous work on DWI of the prostate. A further detriment has been the necessity to use relatively long echo times, thereby reducing the available SNR, to enable the incorporation of the diffusion sensitizing gradients.

The recent advent of commercially available 3.0 T whole body scanners, with an almost 2-fold increase in SNR over 1.5 T systems, enables significant reduction in imaging times while maintaining image quality. By using a 3.0 T whole-body scanner and using parallel imaging techniques, this article seeks to establish that both DWI and DTI of the human prostate can be implemented in a clinically acceptable acquisition time with reasonable in-plane resolution. The aim of this study was to assess the utility of DWI in differential diagnosis in a relatively large group of patients and to conduct preliminary investigations into DTI of the pathologic prostate. By fully quantifying the diffusion tensor, it is suggested that further insight into disease processes within the prostate gland may be obtained.

MATERIALS AND METHODS

All MR examinations were performed on a Signa Excite 3.0 T whole-body scanner (GE Healthcare, Milwaukee, WI) fitted with zoom gradients and an 8-channel torso phased-array coil (USA Instruments Inc, Aurora, OH). Sixty-seven patients were scanned using DWI (median age 65 years; range, 49–80 years) and DTI was then performed on a subset of 26 of these patients (median age 66 years; range, 53–80 years). All patients were referred, for staging of their prostate cancer, because of elevated PSA levels (60 patients) and/or positive histology obtained via transrectal ultrasound guided biopsy or transurethral resection of the prostate (60 patients).

After initial localizing scans, high-resolution T2-weighted images through the pelvis were acquired, for the benefit of organ and lesion visualization. Diffusion-weighted images through the prostate at 7 slice locations were then acquired using spin-echo echo-planar imaging (TE 65.7 milliseconds, TR 4000 milliseconds, 16 averages, slice thickness 5 mm, matrix size 224 × 224, ASSET factor 2, and field of view 26 × 26 cm). The diffusion-encoding gradients were applied as a bipolar pair at *b*-values of 0 and 500 seconds/mm^2, along the y-axis only. Along with DWI, DTI was implemented in 26 cases. Using a dual spin-echo echo-planar imaging sequence, with diffusion gradients applied in 6 different combinations in turn, images were acquired at *b*-values of 0 and 700 seconds/mm^2. Acquisition parameters included TE 64.8 milliseconds, TR 6200 milliseconds, 6 averages, slice thickness 2.7 mm, matrix size 128 × 128, ASSET factor 2, and field of view 35 × 35 cm, resulting in images of in-plane resolution 2.7 × 2.7 mm. The acquisition time was 4.5 minutes for 28 slices through the prostate and surrounding anatomy.

After data acquisition, all images were transferred to an Advantage Windows 2 Workstation for subsequent analysis. Regions of interest (ROIs) were drawn on the $b = 0$ seconds/mm^2 images using the high-resolution T2-weighted images as reference. Hypointense areas in the peripheral zone were regarded as being indicative of prostatic carcinoma whereas hyperintense signal was taken to be normal tissue. Because BPH is known to be prevalent in this age group and there is no reliable way of differentiating BPH from prostatic carcinoma using T2-weighted images, no regions were examined in the central gland. From the DWI data, ADC values in the y-direction were calculated (denoted ADC_y) and from the diffusion tensor images the mean diffusivity, fractional anisotropy, and trace elements (D_{xx}, D_{yy}, D_{zz}) were computed.

Differences between tissue types were explored visually using box and whisker plots and were investigated using the independent samples *t* test or nonparametric equivalent where appropriate. Receiver operating characteristic (ROC) curves were used to determine the diagnostic accuracy of diffusion measurements. Scatter-plots and the Spearman's rho correlation coefficient were used to determine the strength of the relationship between the calculated diffusion parameters and the clinical measures of Gleason score and PSA level.

RESULTS

ADC_y calculations were not possible in 5 patients because of excessive susceptibility artifacts, arising from air filled rectum in 4 cases and the presence of bilateral hip replacements in 1. In a further 11 patients, normal-appearing peripheral zone tissue could not be reliably identified. Therefore, ADC_y values were calculated in prostatic carcinoma for 62 patients and in normal peripheral zone for 51 patients. Biochemistry revealed a median PSA of 9.2 μg/L (range, 1.6–130.0 μg/L) and histopathology revealed a median Gleason score of 7 (range, 2–10) for the study population (illustrated in Fig. 1). Figure 2 illustrates a box-plot of ADC_y values for prostatic carcinoma and normal-appearing peripheral zone tissue. Although a significant difference existed between the 2 groups ($P < 0.0001$) a certain degree of overlap between tissue types was evident. ROC curve anal-

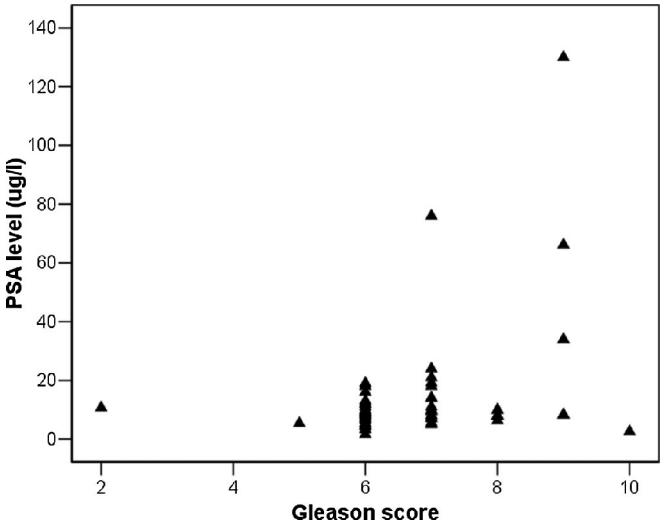

FIGURE 1. Scatter plot of Gleason score against PSA level for the study population.

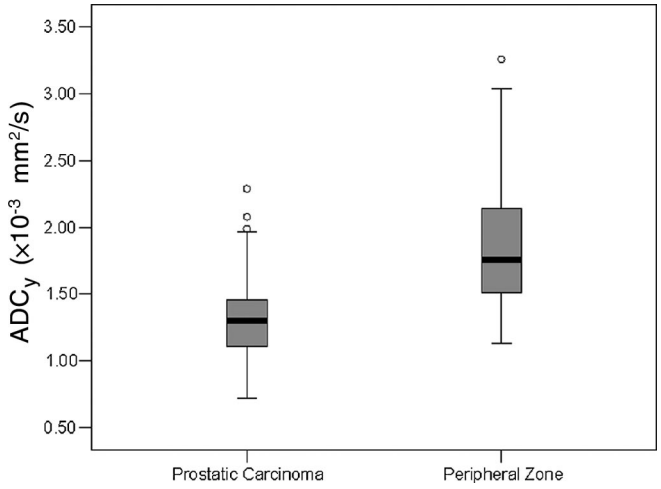

FIGURE 2. Box plot of tissue status against ADC$_y$, obtained from diffusion weighted imaging, demonstrating intersubject variability.

ysis revealed that ADC$_y$ had a diagnostic accuracy (given by the area under the curve) of 0.85 ± 0.04 with a sensitivity of 82% and a specificity of 78% using a cut-off value of 1.50×10^{-3} mm^2/s. There was no evidence of correlation between prostatic carcinoma ADC$_y$ values and either PSA value ($r = -0.037$, $P = 0.779$) or Gleason score ($r = -0.171$, $P = 0.087$).

From the DTI data, analysis was not possible in one case only because of susceptibility artifacts. Normal-appearing peripheral zone tissue could be identified in 20 of the remaining 25 cases. For this subset of the total patient group, a median PSA value of 8.3 μg/L (range, 2.6–130.0 μg/L) and a median Gleason score of 7 (range, 3–9) were noted. The mean, standard deviation, and range of values obtained for all calculated parameters are presented in Table 1. Data from a patient, with an area of reduced signal intensity in the right peripheral zone on the $b = 0$ seconds/mm^2 image, indicative or prostatic carcinoma, is illustrated in Figure 3. Significant differences were noted between normal-appearing peripheral zone tissue and prostatic carcinoma for all diffusion parameters, namely mean diffusivity, D$_{xx}$, D$_{yy}$, D$_{zz}$, and fractional anisotropy ($P < 0.0001$ in all cases), using the independent samples *t* test. Using ROC curve analysis diagnostic accuracy

TABLE 1. Calculated ADC$_y$ and Diffusion Tensor Parameters for All Patients

	Tumor	Peripheral Zone
ADC$_y$ (×10^{-3} mm^2/s)	1.33 ± 0.32 (0.72–2.29)	1.86 ± 0.47 (1.13–3.26)
D$_{xx}$ (×10^{-3} mm^2/s)	1.21 ± 0.29 (0.73–1.83)	1.67 ± 0.24 (1.17–2.17)
D$_{yy}$ (×10^{-3} mm^2/s)	1.13 ± 0.26 (0.67–1.69)	1.61 ± 0.29 (1.12–2.29)
D$_{zz}$ (×10^{-3} mm^2/s)	1.22 ± 0.32 (0.67–2.04)	1.63 ± 0.17 (1.42–1.96)
Mean diffusivity (×10^{-3} mm^2/s)	1.19 ± 0.26 (0.69–1.77)	1.64 ± 0.21 (1.38–2.14)
Fractional anisotropy	0.24 ± 0.05 (0.15–0.37)	0.16 ± 0.06 (0.09–0.28)

Values are quoted as mean ± SD and range in parenthesis.

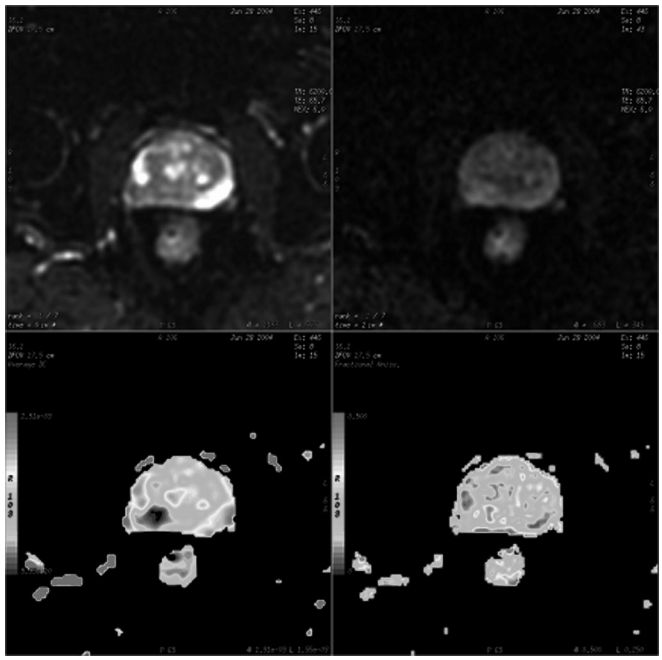

FIGURE 3. Diffusion weighted spin-echo echo-planar images of a patient with prostatic carcinoma with (A) $b = 0$ seconds/mm^2 and (B) $b = 700$ seconds/mm^2. The corresponding mean diffusivity and fractional anisotropy maps are illustrated in (C) and (D), respectively.

varied between 0.83 using fractional anisotropy and 0.93 using mean diffusivity (illustrated in Fig. 4). Using a cut-off value of 1.45×10^{-3} mm^2/s for mean diffusivity resulted in a sensitivity of 84% and a specificity of 80%. No significant

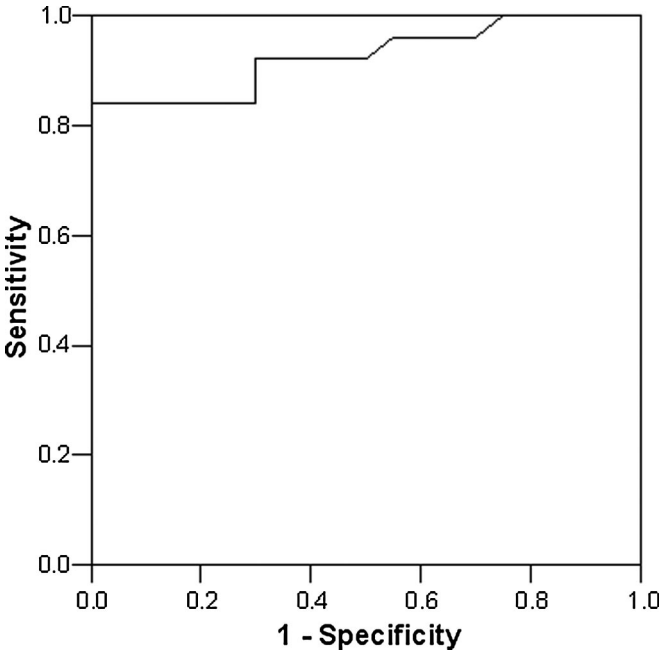

FIGURE 4. ROC curve analysis for mean diffusivity. A diagnostic accuracy (area under the curve) of 0.93 is obtained.

correlations with either PSA levels or Gleason score were noted for all calculated diffusion tensor parameters.

DISCUSSION

In this report, the use of a high magnetic field strength and parallel imaging technology enabled DWI and DTI spanning the prostate and surrounding anatomy to be obtained in clinically acceptable imaging times. An endorectal coil[20] was not used because its use would lead to increased susceptibility effects necessitating a fast spin-echo based imaging sequence.[21] For the DTI, a dual spin-echo echo-planar imaging sequence was applied to reduced eddy currents and consequent image distortions.

Considering the patient results, differences in mean diffusivity and ADC_y between cancerous and noncancerous regions agree with previously published data in which reduced ADC values within cancerous tissue were observed.[14,16] Significant differences also were noted in fractional anisotropy, and the results appear to be in excellent agreement with the preliminary findings of Chen et al,[22] who reported fractional anisotropy values of 0.26 ± 0.08 and 0.18 ± 0.05 in cancerous and noncancerous regions, respectively. However, the degree of overlap evident from Table 1 indicates that no single diffusion parameter was able to fully discriminate between cancerous and noncancerous regions in the prostate.

Initially, the lack of correlation between the calculated diffusion parameters and either PSA or Gleason score may seem problematic. However, PSA level cannot be considered to be a "gold standard" measurement for the detection of prostatic cancer and is prone to some errors. A PSA value greater than 4.0 μg/mL usually is taken to be indicative of cancer but has been shown to have a false-negative rate of as much as 20% and a false-positive rate as high as 65%. All but 2 cases in this study had biopsy-proven cancer. However, Gleason scores also are prone to sampling error.

The results presented herein must be considered in the context of the limitations of the study. As has been widely reported, T2-weighted imaging is not a perfect technique for delineation of prostate cancer.[4–6] It also must be noted that the exclusion of the central gland entails limitations because approximately one-third of prostate cancers arise within this region. The potential use of a cut-off ADC value to indicate prostatic cancer can only be fully explored using radical retropubic prostatectomy specimens. Without such specimens, the potential of diffusion imaging to improve detection of tumor foci above that obtained with T2-weighted imaging is beyond the scope of this work. Finally, bearing in mind that the resolution of the diffusion-weighted images and resulting ADC maps is less than that obtained using conventional imaging sequences it is extremely unlikely they will be used in isolation and will thus primarily provide add-on value.

In conclusion, this study has demonstrated the potential use of diffusion imaging of the prostate at 3.0 T. ADC values have been determined in a large group of patients and the diffusion tensor explored for a subset of these. Reduced ADC values and increased fractional anisotropy appear to be indicative of prostatic carcinoma.

ACKNOWLEDGMENTS

We are grateful to Mr. Adrian Knowles of GE Healthcare for his assistance in imaging protocol development.

REFERENCES

1. American Cancer Society. Cancer facts and figures 2004. Available at http://www.cancer.org/downloads/STT/CAFF_finalPWSecured.pdf. Accessed October 24, 2005.
2. Beduschi M, Oesterling JE. Percent free prostate-specific antigen: the next frontier in prostate-specific antigen testing. *Urology*. 1998;51:98–109.
3. Liney GP, Lowry M, Turnbull LW, et al. Proton MR T2 maps correlate with the citrate concentration in the prostate. *NMR Biomed*. 1996;9:59–64.
4. Quint LE, van Erp JS, Bland PH, et al. Prostate cancer: correlation of MR images with tissue optical density at pathologic examination. *Radiology*. 1991;179:837–842.
5. Sommer FG, Ngjiem HV, Herfkens R, et al. Determining the volume of prostatic carcinoma –value of MR imaging with an external-array coil. *AJR Am J Roentgenol*. 1993;161:81–86.
6. Coakley FV, Kurhanewicz J, Lu Y, et al. Prostate cancer tumour volume: measurement with endorectal MR and MR spectroscopic imaging. *Radiology*. 2002;223:91–97.
7. Padhani AR, Gapinski CJ, MacVicar DA, et al. Dynamic contrast enhanced MRI of prostate cancer: correlation with morphology and tumour stage, histological grade and PSA. *Clin Radiol*. 2000;55:99–109.
8. Kiessling F, Huber PE, Grobholz R, et al. Dynamic magnetic resonance tomography and proton magnetic resonance spectroscopy of prostate cancers in rats treated by radiotherapy. *Invest Radiol*. 2004;39:34–44.
9. Buckley DL, Roberts C, Khaki SK, et al. Characterisation of prostate cancer by quantitative MRI. In: Proc 12th Annual Meeting ISMRM, Kyoto, 2004. p 615.
10. Dodd NFJ, Zhao S. Early detection of tumour response to radiotherapy using MRI. *Phys Med*. 1997;13(Suppl 1):56–60.
11. Jennings D, Hatton BN, Guo J, et al. Early response of prostate carcinoma xenografts to docetaxel chemotherapy monitored with diffusion MRI. *Neoplasia*. 2002;4:255–262.
12. Plaks V, Koudinova N, Nevo U, et al. Photodynamic therapy of established prostatic adenocarcinoma with TOOKAD: a biphasic apparent diffusion coefficient change as potential early MRI response marker. *Neoplasia*. 2004;6:224–233.
13. Gibbs P, Tozer DJ, Liney GP, et al. Comparison of quantitative T2 mapping and diffusion weighted imaging in the normal and pathologic prostate. *Magn Reson Med*. 2001;46:1054–1058.
14. Issa B. In vivo measurement of the apparent diffusion coefficient in normal and malignant prostatic tissues using echo-planar imaging. *J Magn Reson Imaging*. 2002;16:196–200.
15. Chan I, Wells W, Mulkern R, et al. Detection of prostate cancer by integration of line-scan diffusion, T2-mapping and T2-weighted magnetic resonance imaging: a multichannel statistical classifier. *Med Phys*. 2003;30:2390–2398.
16. Hosseinzadeh K, Schwarz SD. Endorectal diffusion-weighted imaging in prostate cancer to differentiate malignant and benign peripheral zone tissue. *J Magn Reson Imaging*. 2004;20:654–661.
17. Pickles MD, Gibbs P, Sreenivas M, et al. Diffusion weighted imaging of normal and pathological prostate tissue at 3.0 T. In: Proc 13th Annual Meeting ISMRM, Miami Beach, 2005. p. 1940.
18. Tozer DJ, Gibbs P, Turnbull LW. Investigation of anisotropy in the prostate using echo planar diffusion weighted imaging. In: Proc 8th Annual Meeting ISMRM, Denver, 2000 p. 1435.
19. Sinha S, Sinha U. In vivo diffusion tensor imaging of the human prostate. *Magn Reson Med*. 2004;52:530–537.
20. Futterer JJ, Scheenen TWJ, Huisman HJ, et al. Initial experience of 3 Tesla endorectal coil magnetic resonance imaging and 1H spectroscopic imaging of the prostate. *Invest Radiol*. 2004;39:671–680.
21. Vigneron DB, Xu D, Chen AP, et al. Diffusion tensor imaging of the prostate using single shot fast spin-echo. In: Proc 10th Annual Meeting ISMRM, Hawaii, 2002. p. 457.
22. Chen AP, Xu D, Henry R, et al. Diffusion tensor imaging of the prostate following therapy. In: Proc 11th Annual Meeting ISMRM, Toronto, 2003. p. 579.